Novel Two- and Three-Dimensional Organometallic−Organic Hybrid Materials Based on Polyphosphorus Complexes

Bianca Attenberger,[†] Eugenia V. Peresypkina,[‡,§] and Manfred Scheer*[,†]

[†]Institut für Anorganische Chemie, Universität Regensburg, Universitätsstrasse 31, Regensburg D-93053, Germany

[‡]Nikolaev Institute of Inorganic Chemistry, Siberian Division of the Russian Academy of Sciences, Lavrentyev prosp. 3, 630090 Novosibirsk, Russia

[§]Novosibirsk State University, Pirogova str. 2, 630090 Novosibirsk, Russia

Ⓢ *Supporting Information*

ABSTRACT: The reaction of the silver salt $Ag[Al\{OC(CF_3)_3\}_4]$ (**1**) with the P_2 ligand complex $[Cp_2Mo_2(CO)_4(\eta^2\text{-}P_2)]$ (**2**) and the organic ditopic linker *trans*-1,2-di(pyridine-4-yl)ethene (*dpe*) results in the formation of four novel organometallic−organic hybrid compounds. Depending on the reaction conditions, the two-dimensional networks $[\{Cp_2Mo_2(CO)_4(\mu_4,\eta^{1:1:2:2}\text{-}P_2)\}(\mu,\eta^{1:1}\text{-}C_{12}H_{10}N_2)Ag]_n[Al\{OC(CF_3)_3\}_4]_n \cdot 0.075n CH_2Cl_2 \cdot 1.425n C_6H_6$ (**3**) and $[\{Cp_2Mo_2(CO)_4(\mu_3,\eta^{2:2:2}\text{-}P_2)\}_2(\mu,\eta^{1:1}\text{-}C_{12}H_{10}N_2)_3Ag_2]_n[Al\{OC(CF_3)_3\}_4]_{2n} \cdot 2n C_7H_8$ (**4**) are accessible. The latter shows a two-dimensional (2D) → 2D interpenetration structure. Furthermore, the formation of a unique three-dimensional polymer $[\{Cp_2Mo_2(CO)_4(\mu_4,\eta^{1:1:2:2}\text{-}P_2)\}(\mu,\eta^{1:1}\text{-}C_{12}H_{10}N_2)Ag]_n[Al\{OC(CF_3)_3\}_4]_n \cdot 0.3n CH_2Cl_2$ (**5b**) together with another 2D polymer $[\{Cp_2Mo_2(CO)_4(\mu_4,\eta^{1:1:2:2}\text{-}P_2)\}(\mu,\eta^{1:1}\text{-}C_{12}H_{10}N_2)_3Ag_2]_n[Al\{OC(CF_3)_3\}_4]_{2n} \cdot 0.75CH_2Cl_2 \cdot 0.5C_7H_8$ (**5a**) was observed. In three of these polymers, unprecedented organometallic nodes were realized including one, two, or even four silver cations. All products were characterized by X-ray structural analysis and classified by the structural characteristics in three different network topologies.
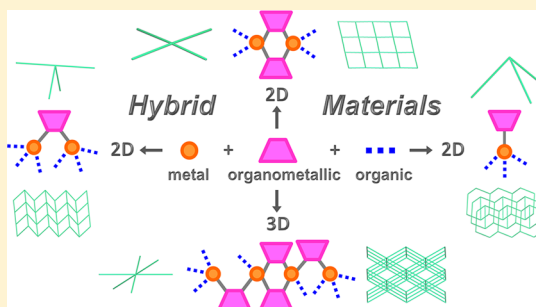
INTRODUCTION

Since metal−organic frameworks (MOF) were discovered by Yaghi in 1995,[1] the rapid growth of interest in the area has followed.[2] According to the criteria of Yaghi's MOF definition, purely inorganic polyatomic moieties are connected by organic linker molecules to form neutral three-dimensional porous networks with a predefined size and volume of the pores. A main difference in comparison to the classical coordination polymers (CPs), besides the wider range of dimensionality [CPs, one-dimensional (1D) to three-dimensional (3D)] and the fact that coordination complexes serve as the nodes (CPs comprising usually single metal ions),[3] is the presence of relatively strong bonds within the metal−organic frameworks.[4] The great potential of this class of metal−organic material is viewed by its use, e.g., for gas storage and separation or in catalysis.[2,5] The rational approach that Yaghi et al. invented for the description of the building process of MOFs is reticular chemistry.[4b,6] Predesigned building units (SBUs) are combined to give defined porous networks. The metal-containing SBUs act therein as connectors (also called "joints" or "nodes") that are associated by the organic linkers acting as "struts" or "spacers".[2a,4−7] In contrast to the variety of known metal−organic materials, only a few organometallic−organic hybrid compounds are described in the literature. F. E. Hahn et al. succeeded, e.g., in the synthesis of molecular rectangles by using N-heterocyclic carbenes constructing the nodes.[8] The

group of K. Severin deals with the construction of metallamacrocyclic compounds, using organometallic half-sandwich complexes of Ru[II], Rh[III], and Ir[III] in combination with organic linkers.[9] A potential use of these metallamacrocyclic compounds is the detection of small molecules. The organometallic−organic hybrid compounds mentioned above represent nonpolymeric aggregates: to the best of our knowledge, no polymeric networks of this type are known besides two examples of 1D and two-dimensional (2D) organometallic−organic hybrid polymers recently reported by our group.[10] By using Ag[I] and Cu[I] salts in combination with the P_2 ligand complex $[Cp_2Mo_2(CO)_4(\eta^2\text{-}P_2)]$ and an organic spacer, coordination polymers are designed. Here lies the special value of the new approach in this field. Because of the arrangement of the linkers, P_n ligand complexes, and metal cations, a large variety of the resulting polymers can be expected. In particular, various mono- and polynuclear nodes (Scheme 1) can be proposed, whereas so far, only dinuclear nodes **A** and **B** have been used.[10,11] The silver derivative contains nodes of type **A**, resulting in a chainlike 1D polymer, whereas the obtained 2D copper-based polymer reveals a layered structure constructed from building block **B** (Scheme 1). The nodes in Scheme 1 differ either by stoichiometry or by

Scheme 1. Proposed Organometallic Subunits of M$_2$P$_2$ Ligand Complexes and n M^I Ions (n = 1−4)^a
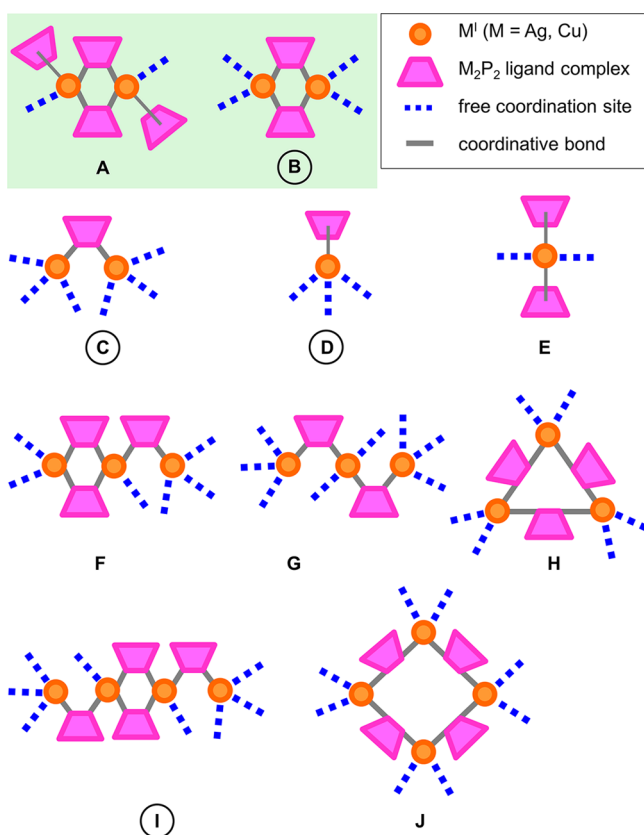
^{a}Nodes **A** and **B** (green highlighted) are known.[10,11] Nodes **C−J** are hypothetical, while circled types **B−D** and **I** are novel and presented in this work (*vide infra*). The selection was limited to tetrahedrally coordinated M^I ions and building blocks that provide the largest number of free coordination sites for the organic linkers.

their coordination abilities and can offer a variable number of potential coordination sites from three (type **D**) to eight (types **I** and **J**). Hence, a wide variety of the topologies and different coordination patterns for coordination polymers based on
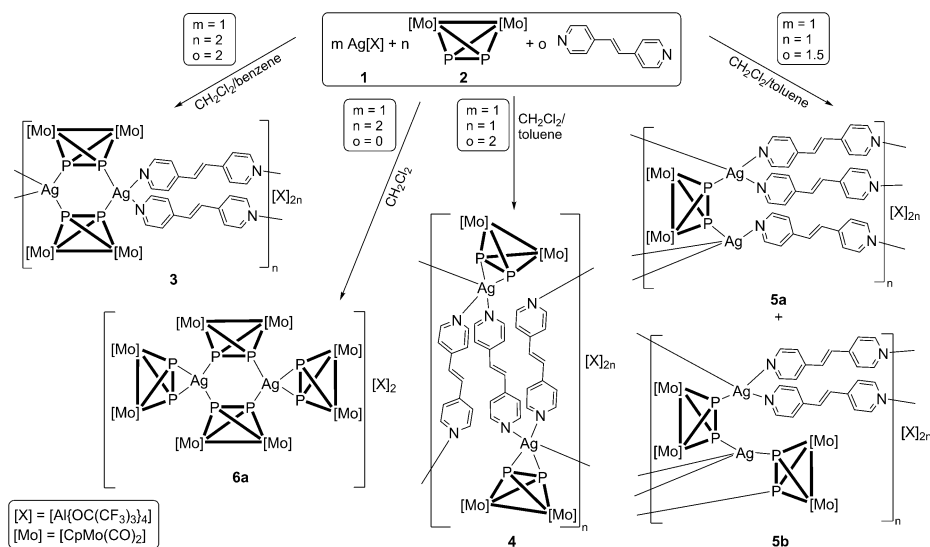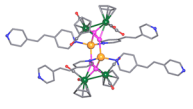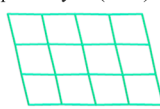
M$_2$P$_2$ complex **2** are available. Just as versatile as the architectures of the polymers is the potential usage of the obtained materials. The hybrid polymers can offer interesting mechanical, electronic, or optical properties depending on the nature of the used building blocks. Establishing organometallic−organic hybrid compounds as a complement to metal−organic analogues might open up new perspectives in organometallic chemistry such as used in gas storage, catalysis, or molecular recognition as the new materials may offer different and synergetic features because of the incorporation of the organometallic building blocks.

Herein, we present the first synthesis and structural characterization of four novel types of polymeric organometallic−organic hybrid aggregates obtained from the silver(I) salt Ag[Al{OC(CF$_3$)$_3$}$_4$] (**1**, Ag[X]) and the organometallic P$_2$ ligand complex [Cp$_2$Mo$_2$(CO)$_4$(η^2-P$_2$)] (**2**) in combination with the organic bipyridyl linkers *trans*-1,2-di(pyridine-4-yl)ethene (*dpe*). They represent three hitherto unknown types of two-dimensional networks, in which polymer **4** shows a unique and, for organometallic−organic frameworks, unprecedented interpenetration of layers in the solid state structure. In addition, we describe the first 3D organometallic−organic hybrid polymer (**5b**). Three more hypothetical organometallic building blocks given in Scheme 1 (see encircled letters) were realized by the novel frameworks of **3**, **4**, and **5a,b**.

RESULTS AND DISCUSSION

The reaction of 1 equiv of Ag[X] (**1**) with 2 equiv of **2** and *dpe* in CH$_2$Cl$_2$ followed by a slow diffusion of benzene leads to the formation of the 2D network [{Cp$_2$Mo$_2$(CO)$_4$(μ_4,$\eta^{1:1:2:2}$-P$_2$)}(μ,$\eta^{1:1}$-C$_{12}$H$_{10}$N$_2$)Ag]$_n$[X]$_n$·0.075nCH$_2$Cl$_2$·1.425nC$_6$H$_6$ (**3**). Using toluene instead of benzene, and using only 1 equiv of the P$_n$ ligand complex **2**, another 2D network [{Cp$_2$Mo$_2$(CO)$_4$(μ_3,$\eta^{2:2:2}$-P$_2$)}$_2$(μ,$\eta^{1:1}$-C$_{12}$H$_{10}$N$_2$)$_3$Ag$_2$]$_n$[X]$_{2n}$·2nC$_7$H$_8$ (**4**) that shows interpenetration in its solid state structure is accessible. A slight change in the stoichiometry of the starting compounds (equimolar ratio of **1** and **2** and 1.5 equiv of *dpe*) leads to the formation of a third 2D aggregate, [{Cp$_2$Mo$_2$(CO)$_4$(μ_4,$\eta^{1:1:2:2}$-P$_2$)}(μ,$\eta^{1:1}$-C$_{12}$H$_{10}$N$_2$)$_3$Ag$_2$]$_n$[X]$_{2n}$·0.75CH$_2$Cl$_2$·0.5C$_7$H$_8$ (**5a**), and even the very first three-

Scheme 2. Syntheses of Compounds 3, 4, 5a,b, and 6a^{11a}

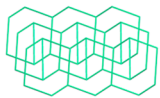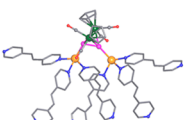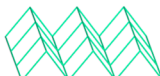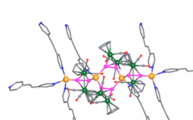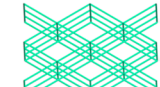**Table 1. Some Geometric Characteristics of the Nodes in 3, 4, and 5a,b and the Resulting Networks**

node and spacer	coordination figure of the node[7b]	dimensionality of the network	topology[4b]
3	square plane	plane layers (0 0 1)	**sql** (Shubnikov tetragonal plane net)
4	Ψ-trigonal pyramid	puckered layers (0 1 0)	**hcb**[a] (Shubnikov hexagonal plane net)
5a	disphenoid	staggered layers (0 1 0)	**sql** (Shubnikov tetragonal plane net)
5b	distorted octahedron	3D framework	**pcu** (α-Po primitive cubic)

[a]Twice-interpenetrated (see text).

dimensional organometallic−organic framework, $[\{Cp_2Mo_2(CO)_4(\mu_4,\eta^{1:1:2:2}\text{-}P_2)\}(\mu,\eta^{1:1}\text{-}C_{12}H_{10}N_2)Ag]_n[X]_n\cdot 0.3nCH_2Cl_2$ (**5b**) (Scheme 2).

Compounds **3**, **4**, and **5a,b** have been characterized by single-crystal X-ray structural analysis (for details, see Table S1 of the Supporting Information). In all crystal structures of the polymers, the nodes are based on Ag^I ions and the P_n ligand complex $[Cp_2Mo_2(CO)_4(\eta^2\text{-}P_2)]$ (**2**), which are cross-linked by the *dpe* spacers.

A detailed overview of the nodes found in **3**, **4**, and **5a,b** as well as the resulting connectivity of a coordination polymers is given in Table 1.

So far, only type **A** and **B** nodes (Scheme 1) were reported to build coordination polymers from P_n ligand complexes and metal(I) salts.[10] The similar nodes of **B**, now based on Ag instead of Cu (Scheme 1), are found in the new 2D network **3**. The connectivity in the building blocks is identical to that of the known copper(I) polymer[10] and the new silver(I) network **3**. Building block **B** consists of two silver cations bridged by two units of P_n ligand complex **2** to form six-membered Ag_2P_4 moieties (Scheme 1, **B**). This is the common heterometallic subunit in coordination compounds of the diphosphorus complex $[Cp_2Mo_2(CO)_4(\eta^2\text{-}P_2)]$ (**2**), which thereby acts as bridging unit.[10,11] In combination with monovalent group 11 cations, together with salts of noncoordinating anions, the dimers of the general composition $[M_2(\{Cp_2Mo_2(CO)_4(\mu,\eta^{2:2}\text{-}P_2)\}_2)(\{Cp_2Mo_2(CO)_4(\mu,\eta^{2:1:1}\text{-}P_2)_2\})][X]_2$ [M = Ag (**6**), Cu, or Au; X = Al{OC(CF$_3$)$_3$}$_4$ (**a**), BF$_4$, ClO$_4$, PF$_6$, or SbF$_6$] are formed.[11a] If copper(I) halides are used, 1D polymeric chains are built up.[11b] The Ag_2P_4 six-membered ring motif is also present in the recently reported discrete and 1D polymeric hybrid compounds[10] with nodes of type **A** (Scheme 1). In **3**, each silver cation of the node has two more free coordination sites accessible for the organic linkers. The number of available coordination sites provided by these nodes is in total four, and their mutual arrangement (or, in other words, the coordination figure[7b]) is a flat square with a shoulder size[12] of 16.5 Å × 15.9 Å (Table 1). In contrast, in **4**, the node represents a

mononuclear Ag^I complex only and is the smallest one in the row [type **D** (Scheme 1)]. The silver cation is η^2 *side-on* coordinated by P_2 ligand complex **2**, which serves as a blocking group. Three vacant positions at the silver ion are available for further coordination to the spacers. The resulting coordination mode is rather unusual, being a trigonal pyramid with a silver cation coordinating the $[Cp_2Mo_2(CO)_4(P_2)]$ (**2**) moiety at the top while the shoulder size is 17.8 Å × 18.6 Å (Table 1). At the same time, it provides higher connectivity for the net because of the small size and a greater number of free coordination sites per silver atom.

The node in polymer **5a** is a binuclear $[Ag_2(\eta^{1:1}\text{-}\mathbf{2})]$ unit [type **C** (Scheme 1)]. Compared to the Ag_2P_4 six-membered ring motif in node **A** or **B** (Scheme 1), one bridging P_n ligand complex **2** is missing in this node **C**. Therefore, each Ag^I bears three coordination sites available for the linkers, and the coordination capability of the entire building block is six. The coordination figure of this building block is disphenoid with a shoulder size of 17.4 Å × 18.5 Å (Table 1).

Finally, polymer **5b** possesses the largest known tetranuclear joint [type **I** (Scheme 1)] whose structure is based on the Ag_2P_4 moiety that is similar to node **B**. In addition, each of the two silver cations in the six-membered ring is bridged by another $[Cp_2Mo_2(CO)_4(\eta^2\text{-}P_2)]$ (**2**) complex with one more silver cation. In total, this node comprises four silver cations and four bridging complexes of **2**. The cations in the six-membered ring have only one free coordination site left for the organic connectors, while the terminal silver atoms still feature three positions available for the linker molecules. In total, the coordination capabilities of the node reach eight spacers and its coordination figure is distorted octahedral with a 19.0 Å × 20.4 Å shoulder size (Table 1).

In all polymers **3**, **4**, and **5a,b**, the silver cations are four-coordinate (Table 1). Whereas in **3** and **5a,b** the Ag^I ions are in a distorted tetrahedral environment, in polymer **4** a pseudotetrahedral coordination geometry is realized. Table 2 shows the comparison of some characteristic bond lengths in the nodes forming the networks of polymers **3**, **4**, and **5a,b**.

Table 2. Comparison of Selected Bond Lengths (angstroms) of the Nodes in Polymers 3, 4, and 5a,b

	3	4	5a	5b
Ag···Ag[a]	4.47, 4.62	–	4.85	4.97,[c] 5.24,[d] 15.3[e]
Ag···Ag[b]	~13.9	~14.0	~13.8	~13.8
Ag−P	2.449(1)− 2.595(1)	2.548(2), 2.610(2)	2.385(2), 2.396(2)	2.477(2)− 2.537(2)
Ag−N	2.278(4)− 2.343(4)	2.316(6)− 2.433(7)	2.283(6)− 2.406(6)	2.303(6)− 2.367(2)
P−P	2.087(2)− 2.091(2)	2.132(3)	2.087(3)	2.085(2), 2.088(2)

[a]Within the node. [b]Between the nodes. [c]In the Ag_2P_4 moiety. [d]In the Ag_2P_2 moiety. [e]The maximal distance within the node (Ag1···Ag4).

The P−P bond lengths in **4−6** vary from 2.085(2) to 2.132(3) Å and are thus slightly elongated compared to those of the noncoordinated complex **2** [2.079(6) Å[13]]. The Ag−P bond lengths [2.385(2)−2.610(2) Å] are in a typical range. The dihedral angles in the Ag_2P_4 six-membered rings amount to 1.44(2)° and 9.52(8)° as well as 7.28(4)° and 9.86(8)°, respectively, in polymer **3** and 1.53(6)° in 3D polymer **5b**. This deviates significantly from the folding angle of 20.69(2)° in the dimeric aggregate [({Cp$_2$Mo$_2$(CO)$_4$(μ,$\eta^{2:2}$-P$_2$)}$_2$)-({Cp$_2$Mo$_2$(CO)$_4$(μ,$\eta^{2:1:1}$-P$_2$)$_2$})Ag$_2$][Al{OC(CF$_3$)$_3$}$_4$]$_2$ (**6a**).[11a]

Because of the similarity of the nodes and the resulting coordination figures, neutral network **3** (Figure 1) is similar to the recently reported analogous Cu^I two-dimensional polymer [Cu{Cp$_2$Mo$_2$(CO)$_4$P$_2$}(dpe)]$_n$[BF$_4$]$_n$.[10] Network **3** differs from the previously described copper(I) polymer[10] of the same connectivity pattern in some of its geometric characteristics because of the different size of the metal atom. For example, the six-membered M_2P_4 ring in the Cu^I polymer is nearly planar [3.61(5)°].[10] The N−M^I−N binding angle to the organic linkers in the known Cu^I compound is much smaller

[110.32(16)°][10] than in polymer **3** [114(15)−121.13(15)°]. In **3**, each silver cation in the organometallic fragments is coordinated by two dpe molecules. Therefore, the resulting framework is 2D polymeric, and the topology of the single layer is the Shubnikov tetragonal plane net (**sql**) (see Table 1 and the Supporting Information); the rhombic meshes show an average size of 12.7 Å × 23.7 Å,[14] while the interlayer distance is ~13.5 Å.[15]

The structure of polymer **4** contrasts markedly with those observed previously for organometallic−organic hybrid materials. The 2D network **4** of puckered hexagons (Figure 2) with Shubnikov hexagonal plane net topology is similar to the puckered sheets in the structure of black phosphorus.[17]

In **4**, for the first time, the well-known six-membered Ag_2P_4 structural motif is missing and the smaller node, [Ag($\eta^{2:2}$-**2**)], is realized instead. Another unique structural feature of polymer **4** is the presence of mechanically independent interlaced layers in the solid state (Figure 3). This phenomenon is called interpenetration and is well-known in the context of MOFs. Interpenetration is defined as the absence of direct connections between sheets, strands, etc., but the separation of the resulting network is not possible without breaking bonds.[18]

With polymer **4**, the first interpenetrated organometallic−organic framework is obtained. Two adjacent layers are interwoven because the long linkers leave enough space in one layer (Figure 3) for the other layer to intergrow. Network **4** can therefore be classified as 2D → 2D parallel interpenetrated[18a] in which the single layers form a two-dimensional framework (Figure 3). The diagonal distances in the meshes of the single layers are ~22.4 Å,[20] while the distances between the interpenetrated sheets and between the pairs of layers are approximately 9.4 and 16.5 Å,[15] respectively.

The counteranions in **4** lie both in the hollows built up from two interwoven layers and between two neighboring interpenetrated pairs of layers.
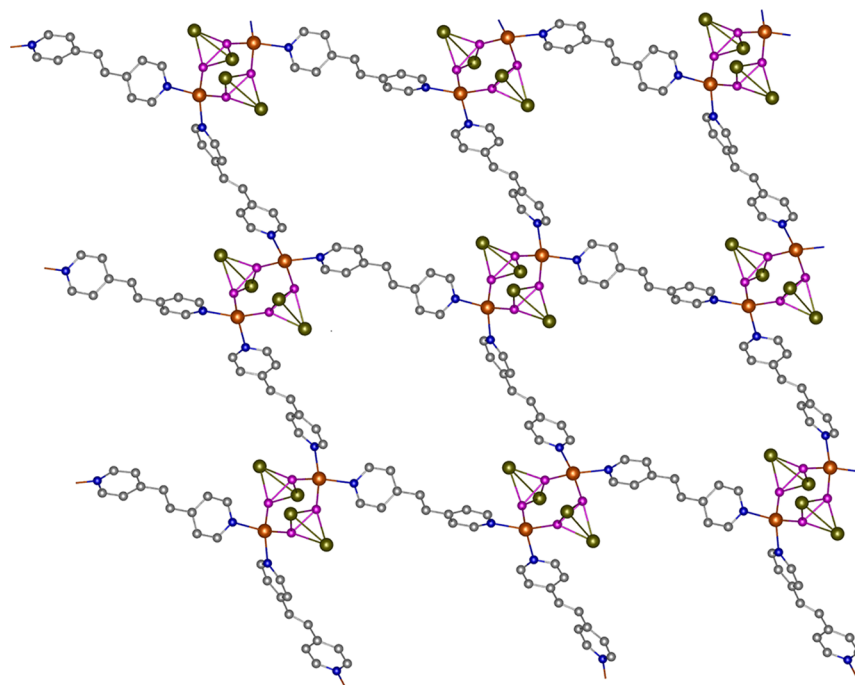

Figure 1. Fragment of a single layer in the 2D polymeric network of **3**. Cp, CO ligands, H atoms, and counteranions have been omitted for the sake of clarity: Ag, orange; P, pink; N, blue; C, gray; Mo, green.[16]
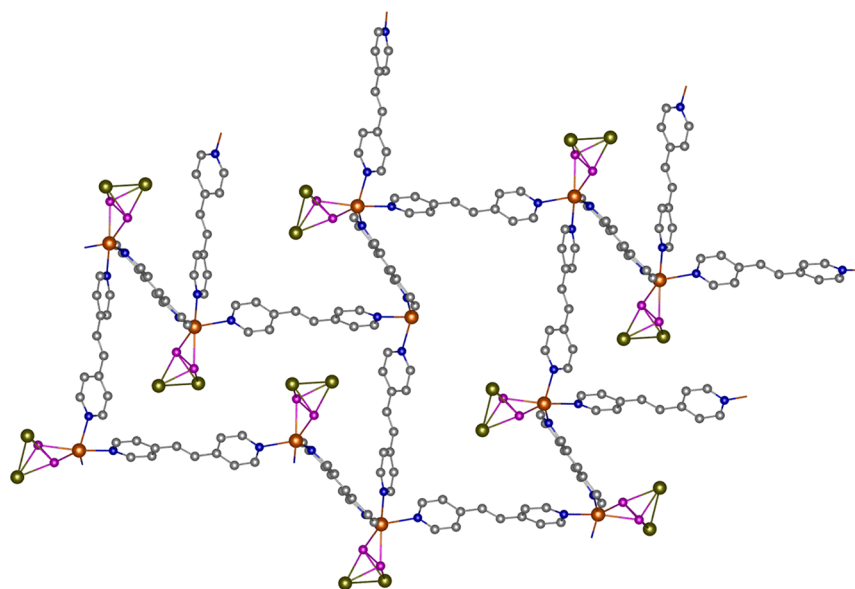
Figure 2. Fragment of a puckered single layer in the 2D polymeric network of **4**. Cp, CO ligands, H atoms, and counteranions have been omitted for the sake of clarity: Ag, orange; P, pink; N, blue; C, gray; Mo, green.[16]
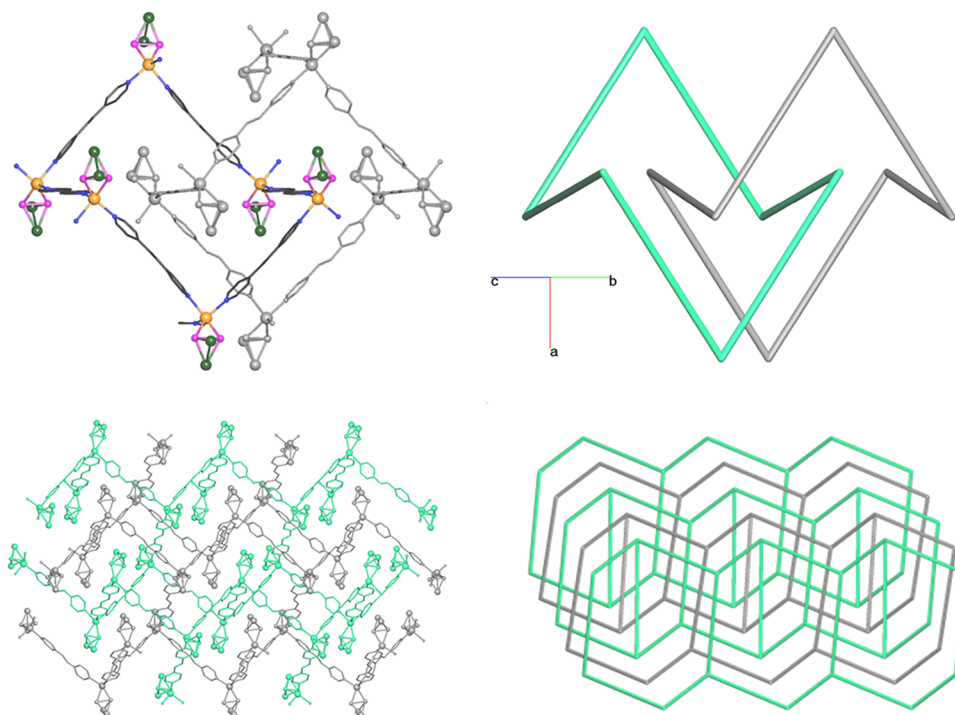

Figure 3. Interpenetration in **4**. Two interwoven six-membered cycles (in chair conformation) in the molecular structure (top left; Ag, orange; P, pink; N, blue; C, gray; Mo, green) and in the simplified net (top right). Schematic view of two interpenetrated 2D sheets in the solid state structure of compound **4** (bottom left) and in the simplified net (bottom right): layer 1, gray; layer 2, green. Cp, CO ligands, H atoms and counteranions have been omitted for the sake of clarity.[19]

The molecular structure of **5a** is depicted in Figure 4; that of **5b** is shown in Figure 5.

The 2D hybrid polymer **5a** consists of four-connected layers similar to **3**, but in **5a**, the layers are staggered. Thus, two kinds of meshes of different size arise: the smaller ones including the P$_2$ ligand complex **2** reveal dimensions of ∼11.4 Å × ∼13.5 Å, whereas the larger ones build up with four molecules of *dpe* and show a size of approximately 18.1 Å × 16.8 Å.[21] The interlayer distances are ∼11.3 Å.[15] The 2D polymeric network in **5a** has **sql**[4b] topology (Table 1) as in compound **3**.

The main difference between **4** and **5a** is that in the former complex **2** coordinates *side-on* while in the latter **2** acts as a bridging unit. However, in both polymers, each silver cation is further linked by three *dpe* ligands. Each Ag^I shows a distorted tetrahedral coordination environment of three nitrogen atoms and one phosphorus atom.

The novel polymer **5b** is the first example of a 3D polymeric organometallic−organic hybrid compound. Another unique feature of polymer **5b** in contrast to **3**, **4**, and **5a** is the presence of two types of silver cations. Though both kinds of silver
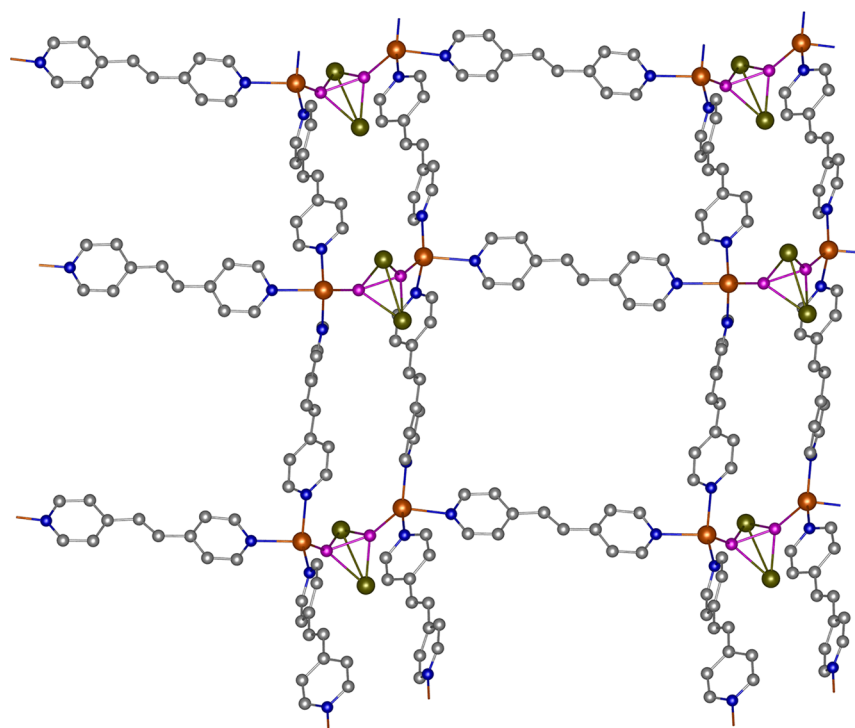
Figure 4. Fragment of one single staggered layer in the 2D polymeric network of **5a**. Cp, CO ligands, H atoms and counteranions have been omitted for the sake of clarity: Ag, orange; P, pink; N, blue; C, gray; Mo, green.[16]
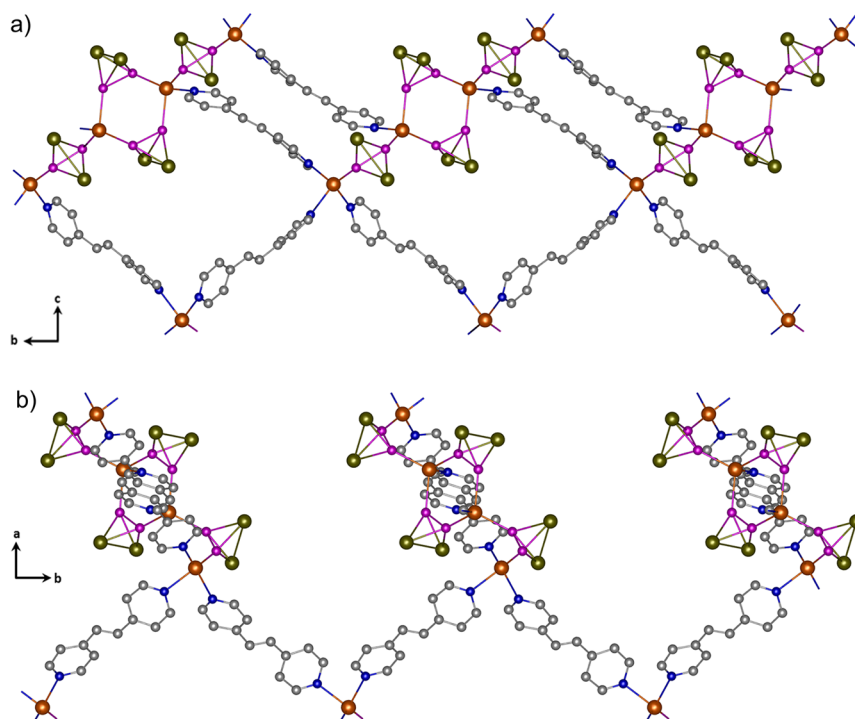

Figure 5. (a) Section of the 3D polymeric network of **5b**, viewed along the crystallographic *a* axis. Cp, CO ligands, H atoms, and counteranions have been omitted for the sake of clarity. (b) Section of the 3D polymeric network of **5b**, viewed along the crystallographic *c* axis. Cp, CO ligands, H atoms, and counteranions have been omitted for the sake of clarity: Ag, orange; P, pink; N, blue; C, gray; Mo, green.[16]

cations are four-coordinate, the silver cations in the Ag_2P_4 moieties are coordinated by three P atoms and one N atom, while the remaining Ag^I ions are conversely surrounded by three N atoms and one P atom. All P_2 ligand complexes **2** in polymer **5b** reveal a bridging coordination mode. The topology of the 3D architecture is primitive cubic (**pcu**)[4b] as in the α-Po

structure. The size of the channels in the framework is ~28.4 Å × 35.0 Å,[22] and they are filled with the bulky aluminate anions.

Interestingly, **3** and **5b** form different networks with the same stoichiometry (1:1:1) of Ag^+, the P_2 ligand complex **2**, and the *dpe* spacers. The syntheses of these products differ by the reaction conditions. For the construction of **3**, the double

stoichiometric amount of ligands **2** and *dpe* was used, while for the synthesis of **5b**, 1 equiv of silver(I) salt **1** and the P_2 ligand complex **2** and 1.5 equiv of *dpe* were provided. During the reaction, CH_2Cl_2 and benzene were used in the synthesis of polymer **3**, whereas in the other case, toluene was used as an aromatic solvent in addition to dichloromethane. Furthermore, polymer **5b** is not exclusively formed, and **5a** was sometimes detected, as well. This result clearly shows that the presented reactions are very sensitive to the reaction conditions as the possibilities for the arrangement of the three starting materials in one compound are versatile. This was also demonstrated in Scheme 1 showing only a small number of potential organometallic building blocks constructed by M^I salts (M = Cu or Ag) and the P_2 ligand complex **2**.

In all the polymeric compounds **3**−**5**, weak interactions between the fluorine atoms of the CF_3 groups of the anions and the protons of the organic ligands *dpe* and/or the Cp units of **2** are present. In the layered compounds **3**, **4**, and **5a**, the single layers (**3** and **5a**) and the interwoven pairs of layers (**4**) are well-separated by the large aluminate anions.

The solubility of all the polymeric compounds **3**, **4**, and **5a,b** in polar solvents like CH_2Cl_2 and CH_3CN is extremely low. Only for polymers **3** and **4** was it possible to perform a complete NMR spectroscopic characterization (^1H, $^{13}C\{^1H\}$, $^{31}P\{^1H\}$, and $^{19}F\{^1H\}$ NMR spectra) in CD_2Cl_2. All expected signals were found in the characteristic regions. A comparison of the chemical shifts in the room-temperature $^{31}P\{^1H\}$ NMR spectra in CD_2Cl_2 shows a shift to a higher field for polymers **3** (δ −88.7) and **4** (δ −80.9) compared to the free P_2 ligand complex **2** (δ −43.2)[11a] and a downfield shift in relation to the linker free dimeric compound $[Ag_2(\{Cp_2Mo_2(CO)_4(\mu,\eta^{2:2}\text{-}P_2)\}_2)(\{Cp_2Mo_2(CO)_4(\mu,\eta^{2:1:1}\text{-}P_2)_2\})][Al\{OC(CF_3)_3\}_4]_2$ (**6a**; δ −96.1).[11a] At least a partial depolymerization of the structures in solution is very likely and is in agreement with the features in the $^{31}P\{^1H\}$ NMR spectra. The base peak in the ESI mass spectra of **3** as well as **4** can be assigned to the fragment $[Ag\{2\}]^+$.

So far, the new hybrid polymers **5a** and **5b** could not be synthesized separately. Besides the formation of the crystalline compounds **5a** and **5b**, a large amount of amorphous material is formed. Because of the low but very similar solubility of crystalline compounds **5a** and **5b**, only a mechanical separation in the glovebox was conducted. The formed amorphous material in the syntheses of **5a** and **5b** was characterized by NMR and IR spectroscopy even if it is almost insoluble in all common solvents. The ^1H NMR spectrum recorded in CD_3CN reveals all expected signals for the linker *dpe*. The $^{31}P\{^1H\}$NMR spectrum shows no signal. In the cationic mode of the ESI mass spectrum, only fragments that do not contain the P_2 ligand complex **2** can be assigned. Most probably, the noncrystalline powder represents coordination polymers of silver(I) and the *dpe* ligand and is free from the P_2 ligand complex **2**, which was additionally proven by the absence of CO bands in the IR spectrum of this solid.

CONCLUSIONS

In conclusion, we succeeded in synthesizing four novel organometallic−organic hybrid polymers **3**, **4**, **5a**, and **5b** from the reaction of the monovalent silver salt Ag[Al{OC-$(CF_3)_3\}_4]$ (**1**) and the organometallic P_2 ligand complex $[Cp_2Mo_2(CO)_4(\eta^2\text{-}P_2)]$ (**2**) in the presence of the organic bipyridyl ligand *dpe*. In the 2D network of **3**, a coordination pattern of the Ag^I-containing node was found, which is similar

to a motif found previously in a copper-based 2D polymer.[10] However, in all other aggregates **4**, **5a**, and **5b**, unprecedented organometallic building blocks showing novel structural topologies in the resulting hybrid networks were found. With the 2D aggregate **4**, a unique interpenetrated hybrid compound was obtained on the basis of the smallest known organometallic node. Finally, besides another novel 2D polymeric network of **5a**, the synthesis of the first-ever three-dimensional organo-metallic−organic hybrid polymer **5b** was successful, the structure of which is based on an organometallic node containing even four silver cations. All compounds were characterized by single-crystal X-ray structural analysis. Hence, the use of the P_2 ligand complexes in the formation of hybrid polymers leads to new bonding features of the resulting porous coordination networks. Thus, a large number of architectures with different topologies based on diverse coordinated organometallic nodes self-assembled by the same starting materials are accessible. Recent experiments in this field focus on the selective and controlled synthesis and the use of different ligands and counteranions forming neutral aggregates with the possibility of tuning the size of the pores to establish the novel organometallic−organic hybrid materials in addition to the already established class of MOF materials.

■ EXPERIMENTAL SECTION

Details of Synthesis. *General Remarks.* All experiments were performed under an atmosphere of dry nitrogen or argon using Schlenk and glovebox techniques. Solvents were freshly distilled under nitrogen from Na/K alloy (*n*-pentane), from Na (benzene/toluene), or from CaH_2 (CH_2Cl_2). IR spectra were recorded on a Varian FTS-800 spectrometer. For ESI-MS measurements, a Finnigan Thermo-quest TSQ 7000 mass spectrometer was used. ^1H, ^{13}C, ^{31}P, and ^{19}F NMR spectra were recorded at room temperature on a Bruker Avance 300 or Avance 400 spectrometer. ^1H, ^{13}C, ^{31}P, and ^{19}F NMR chemical shifts are reported in parts per million relative to external standards Me_4Si, H_3PO_4 (85%), and $CFCl_3$. NMR labeling of the *dpe* (**3**) is used as shown below (Scheme 3).

Scheme 3. Labeling of the *dpe* Ligand
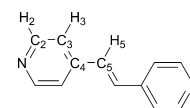
Reagents. *trans*-1,2-Di(pyridine-4-yl)ethene (*dpe*) was purchased from Sigma-Aldrich and used as received. Ag[Al{OC(CF_3)_3\}_4] (**1**)[23] and $[Cp_2Mo_2(CO)_4P_2]$ (**2**)[13,24] were synthesized as reported in the literature.

*Synthesis of $[\{Cp_2Mo_2(CO)_4(\mu_4,\eta^{1:1:2:2}\text{-}P_2)\}_2(\mu,\eta^{1:1}\text{-}C_{12}H_{10}N_2)_2Ag_2]_n[Al\{OC(CF_3)_3\}_4]_{2n}$ (**3**).* A solution of Ag[Al{OC-$(CF_3)_3\}_4]$ (**1**; 35 mg, 0.03 mmol) and 2 equiv each of $[Cp_2Mo_2(CO)_4P_2]$ (**2**; 30 mg, 0.06 mmol) and *dpe* (11 mg, 0.06 mmol) in CH_2Cl_2 (10 mL) were stirred for 3.5 h at ambient temperature in the dark (to avoid Ag formation). Afterward, the mixture was filtered and washed with 2 mL of CH_2Cl_2, and pure benzene (~6 mL) was layered above the obtained red solution. In 1 week, single crystals of **3**·0.075CH_2Cl_2·1.425C_6H_6 suitable for single-crystal X-ray structural analysis formed. These crystals were isolated by filtration, washed with *n*-pentane (2 × 2 mL), and dried in vacuum. Yield: 12 mg (46%). ^1H NMR (CD_2Cl_2, 400 MHz): δ 5.34 (s, C_5H_5), 7.32 (s, 2 H; H_5), 7.36 (s, 2 H; C_6H_6), 7.53 (m, 4 H; H_3), 8.60 (m, 4 H; H_2). $^{13}C\{^1H\}$ NMR (CD_2Cl_2, 101 MHz): δ 87.8 (s; C_5H_5), 121.7 (q, $^1J_{FC}$ = 293 Hz; CF_3), 122.4 (s; C_3), 128.7 (s; C_6H_6), 131.6 (s; C_5), 145.4 (s; C_4), 150.1 (s; C_2), 222.9 (s; CO). $^{31}P\{^1H\}$ NMR (CD_2Cl_2, 162 MHz): δ −88.7 (br s, $\omega_{1/2} \approx$ 125.5 Hz). $^{19}F\{^1H\}$ NMR (CD_2Cl_2, 282 MHz): δ −75.6 (s). Positive ion ESI-MS (CH_2Cl_2): *m/z* (%)

1571.6 (2) $[Ag_2(2)_2(dpe)_2]^+$, 1333.0 (18) $[(dpe)_2(Al\{OC(CF_3)_3\}_4) + H]^+$, 1100.6 (100) $[Ag(2)_2]^+$. Negative ion ESI-MS (CH_2Cl_2): m/z (%) 967.0 (100) $[Al\{OC(CF_3)_3\}_4]^-$.

Synthesis of $[\{Cp_2Mo_2(CO)_4(\mu_3,\eta^{2:2:2}\text{-}P_2)\}_2(\mu,\eta^{1:1}\text{-}C_{12}H_{10}N_2)_3Ag_2]_n[Al\{OC(CF_3)_3\}_4]_{2n}$ *(4)*. $Ag[Al\{OC(CF_3)_3\}_4]$ (**1**; 35 mg, 0.03 mmol) and 2 equiv of $[Cp_2Mo_2(CO)_4P_2]$ (**2**; 30 mg, 0.06 mmol) were dissolved in CH_2Cl_2 (10 mL) and stirred for 3 h at room temperature in the absence of light. After filtration, the red solution was layered with a solution of 2 equiv of *dpe* (11 mg, 0.06 mmol) in toluene (5 mL) using a Teflon capillary. Over the next 3 days, besides some noncrystalline brown powder crystals of compound $4 \cdot 2C_7H_8$ appropriate for single-crystal X-ray structural analysis were obtained. To isolate the crystals, the mother liquor was decanted, washed with *n*-pentane (2 × 2 mL), and dried under vacuum. Yield: 30 mg (54%). ^{1}H NMR (CD_2Cl_2, 400 MHz): δ 5.34 (s; C_5H_5), 7.34 (s, 2 H; H_5), 7.54 (m, 4 H; H_3), 8.61 (m, 4 H; H_2). $^{13}C\{^1H\}$ NMR (CD_2Cl_2, 101 MHz): δ 87.6 (s; C_5H_5), 122.2 (s; C_3), 131.6 (s; C_5), 149.7 (s; C_2). $^{31}P\{^1H\}$ NMR (CD_2Cl_2, 162 MHz): δ −80.9 (br s, $\omega_{1/2} \approx 302.5$ Hz). $^{19}F\{^1H\}$ NMR (CD_2Cl_2, 282 MHz): δ −75.6 (s). Positive ion ESI-MS (CH_2Cl_2): m/z (%) 2357.7 (1) $[Ag_2(2)_2(dpe)(Al\{OC(CF_3)_3\}_4)]^+$, 1333.1 (19) $[(dpe)_2(Al\{OC(CF_3)_3\}_4) + H]^+$, 1100.6 (100) $[Ag(2)_2]^+$, 645.7 (63) $[Ag(2)(CH_3CN)]^+$. Negative ion ESI-MS (CH_2Cl_2): m/z (%) 967.0 (100) $[Al\{OC(CF_3)_3\}_4]^-$.

Synthesis of $[\{Cp_2Mo_2(CO)_4(\mu_4,\eta^{1:1:2:2}\text{-}P_2)\}(\mu,\eta^{1:1}\text{-}C_{12}H_{10}N_2)_3Ag_2]_n[Al\{OC(CF_3)_3\}_4]_{2n}$ *(5a)* *and* $[\{Cp_2Mo_2(CO)_4(\mu_4,\eta^{1:1:2:2}\text{-}P_2)\}(\mu,\eta^{1:1}\text{-}C_{12}H_{10}N_2)Ag]_n[Al\{OC(CF_3)_3\}_4]_n$ *(5b)*. To the stirred red solution of $Ag[Al\{OC(CF_3)_3\}_4]$ (**1**; 35 mg, 0.03 mmol) and $[Cp_2Mo_2(CO)_4P_2]$ (**2**; 15 mg, 0.03 mmol) in CH_2Cl_2 (8 mL) was added dropwise a colorless solution of *dpe* (8 mg, 0.045 mmol) in CH_2Cl_2 (3 mL), and a slight turbidity ensued. After being stirred for 1 h at ambient temperature, the reaction mixture was filtered and overlaid with pure toluene. The immediate occurrence of an amorphous solid, which could not be identified, was observed. Over the next 3 weeks, crystals of **5a** and **5b** suitable for single-crystal X-ray structural analysis were formed besides the mentioned powder. The crystals of $5a \cdot 0.75CHCl_3 \cdot 0.5C_7H_8$ and $5b \cdot 0.3CH_2Cl_2$ were isolated by filtration, washed with *n*-pentane (2 × 2 mL), and dried under vacuum. Yield of **5a** and **5b**: 12 mg (23%). Characterization of the amorphous main product. ^{1}H NMR (CD_3CN, 400 MHz): δ 7.65 (s, 2 H; H_5), 7.84 (m, 4 H; H_3), 8.65 (m, 4 H; H_2). $^{19}F\{^1H\}$ NMR (CD_3CN, 282 MHz): δ −74.7 (s). Positive ion ESI-MS (CH_3CN): m/z (%) 1333.2 (1) $[(dpe)_2(Al\{OC(CF_3)_3\}_4) + H]^+$, 1233 (1) $[(dpe)_2(Al\{OC(CF_3)_3\}_4)(CH_3CN)_2 + H]^+$, 1192.2 (1) $[(dpe)_2(Al\{OC(CF_3)_3\}_4)(CH_3CN) + H]^+$, 1151.1 (1) $[(dpe)_2(Al\{OC(CF_3)_3\}_4) + H]^+$, 224.1 (12) $[(dpe)(CH_3CN)]^+$, 183.0 (100) $[dpe]^+$, 133.0 (12) $[(dpe)(CH_3CN)_2 + H]^{2+}$, 112.5 (8) $[(dpe)(CH_3CN) + H]^{2+}$. Negative ion ESI-MS (CH_2Cl_2): m/z (%) 967.0 (100) $[Al\{OC(CF_3)_3\}_4]^-$.

Crystallographic Details. Single crystals suitable for single-crystal X-ray diffraction analysis were obtained for derivatives **3**, **4**, and **5a,b**. Single-crystal data were collected on an Agilent Technologies SuperNova diffractometer with Cu Kα radiation (λ = 1.54178 Å). The data were processed with CrysAlis.[25] The structures were determined by direct methods with SHELXS.[26] The SHELXL program or its multi-CPU version[26] was used to refine the structures by full-matrix least squares on F^2. All non-hydrogen atoms except for some disordered ones were refined in an anisotropic approximation. Hydrogen atoms were refined isotropically in idealized positions riding on pivot atoms.

One of two independent $[Cp_2Mo_2(CO)_4(\eta^2\text{-}P_2)]$ (**2**) units in **5b** is disordered over two positions so that positions of P_2, one Cp, and one carbonyl group coincide, and Cp and the other CO group are disordered with a 0.75/0.25 ratio. The aluminate anion has a strong tendency to be disordered in crystal structures. In **3**, **4**, **5a**, and **5b**, the anions are disordered in a different way, caused by rotation of either CF_3 or *tert*-$C(CF_3)_3$ groups.[27] It was not always possible to refine the disorder over two or more close positions without using geometrical constraints and restraints (DFIX or/and SADI instructions in SHELX) as well as isotropic or restrained (EADP) displacement parameters. Minor positions of *tert*-$C(CF_3)_3$ groups in **5a** with a relative weight of 0.2 were not included in the model because it was not possible to

refine them. Solvent CH_2Cl_2 (**3**, **5a**, and **5b**) molecules are disordered over two (**3** and **5a**) or three (**5b**) positions. Solvated toluene molecules (**5a**) are disordered over two positions.

A summary of the crystallographic data is given in Table S1 of the Supporting Information. Figures S1−S4 (see the Supporting Information) contain color drawings with detailed information about relevant bond lengths and angles. CCDC reference numbers 1056773, 1056774, 1056775, and 1056776 contain the supplementary crystallographic data for **3**, **4**, **5a**, and **5b**, respectively. These data can be obtained free of charge at www.ccdc.cam.ac.uk/conts/retreving.html or from the Cambridge Crystallographic Data Center, 12 Union Road, Cambridge CB2 1EZ, U.K. Fax: (internat.) +44-1223-336-033. E-mail: deposit@ccdc.cam.ac.uk. The analysis of topological features in crystal structures **3**, **4**, and **5a,b** was performed using ToposPro.[19]

■ ASSOCIATED CONTENT

Ⓢ Supporting Information

X-ray crystallographic data in CIF format, additional structural figures, and bond lengths and angles. The Supporting Information is available free of charge on the ACS Publications website at DOI: 10.1021/acs.inorgchem.5b01048.

■ AUTHOR INFORMATION

Corresponding Author
*E-mail: manfred.scheer@chemie.uni-regensburg.de.

Notes
The authors declare no competing financial interest.

■ ACKNOWLEDGMENTS

■ DEDICATION

Dedicated to Professor Maurizio Peruzzini on the occasion of his 60th birthday.

■ REFERENCES

(1) (a) Yaghi, O. M.; Li, G.; Li, H. *Nature* **1995**, *378*, 703−706. (b) Yaghi, O. M.; Li, H. *J. Am. Chem. Soc.* **1995**, *117*, 10401−10402.

(2) (a) Furukawa, H.; Cordova, K. E.; O'Keeffe, M.; Yaghi, O. M. *Science* **2013**, *341*, 975−986. (b) Foo, M. L.; Matsuda, R.; Kitagawa, S. *Chem. Mater.* **2014**, *26*, 310−322. (c) Janiak, C.; Vieth, J. K. *New J. Chem.* **2010**, *34*, 2366−2388. (d) Kitagawa, S.; Kitaura, R.; Noro, S.-i. *Angew. Chem., Int. Ed.* **2004**, *43*, 2334−2375.

(3) (a) Perry, J. J., IV; Perman, J. A.; Zaworotko, M. J. *Chem. Soc. Rev.* **2009**, *38*, 1400−1417. (b) Robin, A. Y.; Fromm, K. M. *Coord. Chem. Rev.* **2006**, *250*, 2127−2157. (c) Cook, T. R.; Zheng, Y.-R.; Stang, P. J. *Chem. Rev.* **2013**, *113*, 734−777.

(4) (a) Tranchemontagne, D. J.; Mendoza-Cortes, J. L.; O'Keeffe, M.; Yaghi, O. M. *Chem. Soc. Rev.* **2009**, *38*, 1257−1283. (b) O'Keeffe, M.; Peskov, M. A.; Ramsden, S. J.; Yaghi, O. M. *Acc. Chem. Res.* **2008**, *41*, 1782−1789.

(5) Wang, C.; Liu, D.; Lin, W. *J. Am. Chem. Soc.* **2013**, *135*, 13222−13234.

(6) Yaghi, O. M.; O'Keeffe, M.; Ockwig, N. W.; Chae, H. K.; Eddaoudi, M.; Kim, J. *Nature* **2003**, *423*, 705−714.

(7) (a) Li, M.; Li, D.; O'Keeffe, M.; Yaghi, O. M. *Chem. Rev.* **2014**, *114*, 1343−1370. (b) Ockwig, N. W.; Delgado-Friedrichs, O.; O'Keeffe, M.; Yaghi, O. M. *Acc. Chem. Res.* **2005**, *38*, 176−182.

(8) (a) Hahn, F. E.; Radloff, C.; Pape, T.; Hepp, A. *Chem.—Eur. J.* **2008**, *14*, 10900−10904. (b) Hahn, F. E.; Radloff, C.; Pape, T.; Hepp, A. *Organometallics* **2008**, *27*, 6408−6410. (c) Radloff, C.; Hahn, F. E.; Pape, T.; Frohlich, R. *Dalton Trans.* **2009**, 7215−7222. (d) Schmidtendorf, M.; Pape, T.; Hahn, F. E. *Angew. Chem., Int. Ed.* **2012**, *51*,

2195−2198. (e) Schmidtendorf, M.; Pape, T.; Hahn, F. E. *Dalton Trans.* **2013**, *42*, 16128−16141.

(9) (a) Severin, K. *Coord. Chem. Rev.* **2003**, *245*, 3−10. (b) Severin, K. *Chem. Commun.* **2006**, 3859−3867. (c) Mirtschin, S.; Slabon-Turski, A.; Scopelliti, R.; Velders, A. H.; Severin, K. *J. Am. Chem. Soc.* **2010**, *132*, 14004−14005. (d) Kilbas, B.; Mirtschin, S.; Riis-Johannessen, T.; Scopelliti, R.; Severin, K. *Inorg. Chem.* **2012**, *51*, 5795−5804. (e) Kilbas, B.; Mirtschin, S.; Scopelliti, R.; Severin, K. *Chem. Sci.* **2012**, *3*, 701−704. (f) Schouwey, C.; Scopelliti, R.; Severin, K. *Chem.—Eur. J.* **2013**, *19*, 6274−6281.

(10) Attenberger, B.; Welsch, S.; Zabel, M.; Peresypkina, E.; Scheer, M. *Angew. Chem., Int. Ed.* **2011**, *50*, 11516−11519.

(11) (a) Scheer, M.; Gregoriades, L. J.; Zabel, M.; Bai, J.; Krossing, I.; Brunklaus, G.; Eckert, H. *Chem.—Eur. J.* **2008**, *14*, 282−295. (b) Bai, J.; Leiner, E.; Scheer, M. *Angew. Chem., Int. Ed.* **2002**, *41*, 783−786.

(12) Shoulder size is defined here as the minimal distances between Ag^I of neighboring nodes in the net.

(13) Scherer, O. J.; Sitzmann, H.; Wolmershäuser, G. *J. Organomet. Chem.* **1984**, *268*, C9−C12.

(14) Calculated as the average from the diagonal distances between Ag^+ ions minus the doubled ionic radius of Ag^+ ions for coordination number 4 (1.14 Å); distances used for average calculation were 23.2623(7), 24.0498(8), 23.2467(7), 24.1141(8), 12.5606(6), and 12.8421(6) Å.

(15) The shortest distance between two Ag^+ ions in different layers is given.

(16) The drawings were generated with Diamond 3.0 and rendered with POV-Ray 3.6.

(17) (a) Brown, A.; Rundqvist, S. *Acta Crystallogr.* **1965**, *19*, 684−685. (b) Lange, S.; Schmidt, P.; Nilges, T. *Inorg. Chem.* **2007**, *46*, 4028−4035. (c) Köpf, M.; Eckstein, N.; Pfister, D.; Grotz, C.; Krüger, I.; Greiwe, M.; Hansen, T.; Kohlmann, H.; Nilges, T. *J. Cryst. Growth* **2014**, *405*, 6−10.

(18) (a) Batten, S. R. *CrystEngComm* **2001**, *3*, 67−72. (b) Batten, S. R.; Neville, S. M.; Turner, D. R. *Interpenetration. Coordination Polymers: Design, Analysis and Application*; The Royal Society of Chemistry: Cambridge, U.K., 2009; pp 59−95. (c) Batten, S. R.; Robson, R. *Angew. Chem., Int. Ed.* **1998**, *37*, 1460−1494. (d) Blatov, V. A.; Carlucci, L.; Ciani, G.; Proserpio, D. M. *CrystEngComm* **2004**, *6*, 378−395.

(19) Blatov, V. A.; Shevchenko, A. P.; Proserpio, D. M. *Cryst. Growth Des.* **2014**, *14*, 3576−3586. ToposPro is available at http://www.topospro.com.

(20) Calculated as the average from the diagonal distances between Ag^+ ions within one mesh minus the doubled ionic radius of Ag^+ for coordination number 4 (1.14 Å); distances used for average calculation were 23.1800(8), 22.3682(9), and 21.5040(9) Å.

(21) Diagonal distances between Ag^+ ions minus the doubled ionic radius of Ag^+ for coordination number 4 (1.14 Å) are given.

(22) The largest diagonal distances between Ag^+ in a channel are given.

(23) Krossing, I. *Chem.—Eur. J.* **2001**, *7*, 490−502.

(24) Scherer, O. J.; Schwalb, J.; Sitzmann, H. *Inorg. Synth.* **1990**, *27*, 224−227.

(25) *CrysAlis PRO*; Agilent Technologies Ltd.

(26) (a) Sheldrick, G. M. *SHELX97, Program for the Refinement of Crystal Structures*; University of Göttingen: Göttingen, Germany, 1997. (b) Sheldrick, G. M. *Acta Crystallogr.* **2008**, *A64*, 112−122.

(27) (a) Krossing, I.; Reisinger, A. *Coord. Chem. Rev.* **2006**, *250*, 2721−2744. (b) Welsch, S. Complex of monovalent earth- and coin-metal cations with phosphorated ligands. Ph.D. Dissertation, University of Regensburg, Regensburg, Germany, 2011.